FUDMA Journal of Sciences (FJS)
ISSN online: 2616-1370
ISSN print: 2645 - 2944
Vol. 3 No. 2, June, 2019, pp 226 - 231

OPTICAL PROPERTIES OF REDUCED GRAPHENE OXIDE ON IRON OXIDE NANOPARTICLES

[1*]Bala, D. A., [1]Ali, H., [1]Eli, D. and [2]Yunana, T.

[1]*Department of Physics, Nigerian Defence Academy, Kaduna, Nigeria*
[2]*Department of Physics, Kaduna State College of Education Gidan Waya, Nigeria*

*Corresponding Author's Email: dennisbala33@gmail.com

ABSTRACT

In this study, we have successfully synthesized iron oxide/reduced graphene oxide (Fe_3O_4/rGO) nanocomposite materials using a simple, friendly, cost-effective and non-toxic chemical method at room temperature. From the results, the absorbance spectrum of Fe_3O_4/rGO has demonstrated a redshift to higher wavelength when compared to Fe_3O_4 spectrum. This indicates an increase in visible light absorption which could be attributed to the formation of chemical bond between Fe_3O_4 nanoparticles and rGO. The results offer a possible method to dramatically enhance the optical absorption and photocatalytic activity of materials by employing rGO nanostructures and also provide further insight into the development of ideal functionality for future optoelectronic systems.

Keywords: Fe_3O_4 nanoparticles, graphene, photocatalytic, nanocomposite

INTRODUCTION

Functional hybridized materials, due to their versatile structures and unique integrated properties have been used in a diverse range of applications such as energy storage and environmental treatment (Singh et al., 2011, Kemp et al., 2013, Maiti et al., 2014). During the last decade, graphene, a prominently one-atom-thick carbon material has become a new favorite to fabricate functional hybridized materials (Novoselov et al., 2004, Li et al., 2010).

As expected, because of the various connection sites (carboxylic acid, phenol hydroxyl and epoxide groups) and high surface area, the planar graphene oxide (GO) and reduced graphene oxide (rGO) sheets can possess superior adsorption capacity (Hummers and Offeman, 1958, Liu et al., 2014).

Normally, Graphene-based composites incorporated by inorganic nanoparticles (NPs) have been an optimal choice: among these NPs, paramagnetic Fe_3O_4 is a good candidate, which has benefited from its satisfactory magnetic recyclability, low cost and small environmental impact (Li et al., 2010, Laurent et al., 2008, Wu et al., 2013, Wang et al., 2013, Metin et al., 2014).

However, surface modification is a necessary requirement to be able to change the properties of the nanoparticles.

In this study, 3D Fe_3O_4/rGO have been fabricated via spin coating procedure which have macroporous framework of iron oxide NPs with uniform deposition of rGO sheets. Three-dimensional (3D) graphene with interconnected mesoporous network, allowing access and diffusion of ions and molecules, seems to be a good candidate and support for iron oxide Fe_3O_4 NPs. It was found that Fe_3O_4/rGO as self-supported structure shows excellent capability in optical properties. Additionally, our results have confirmed that the addition of rGO on Fe_3O_4 can enhance the optical properties of Fe_3O_4.

MATERIALS AND METHOD

Preparation of Graphene Oxide

The graphene oxide was synthesized from graphite utilizing the modified Hummer's technique (Hummers and Offeman, 1958), called the Tour's Method as demonstrated in Figure 1:

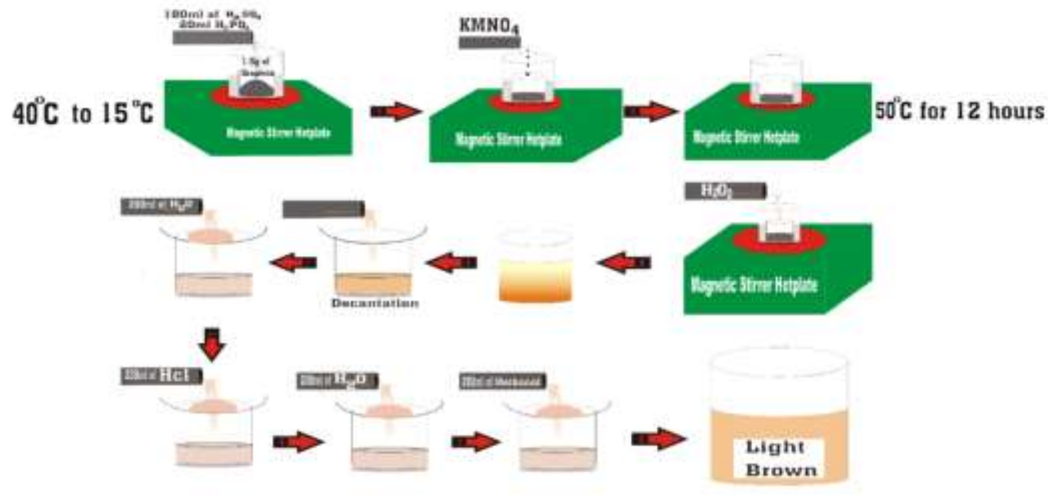

Fig. 1 Schematic representation of the Graphene synthesis

Preparation of Fe_3O_4 Nanoparticles

Fe_3O_4 nanoparticles were prepared using a simple chemical coprecipitation method (Song et al., 2007). Typically, 0.15 mol of $FeCl_2.4H_2O$ and 0.30 mol of $FeCl_3 \cdot 6H_2O$ were freshly prepared in aqueous HCl (2 M), respectively. Both $FeCl_2.4H_2O$ and $FeCl_3.6H_2O$ aqueous solution were then added rapidly to 20 ml of distilled water under nitrogen flow at 80^{o}C with the mixture being continuously stirred under nitrogen. Upon adding an aqueous NH_4OH solution (28%, 4 ml), a distinctive black precipitate of Fe_3O_4 nanoparticles was formed immediately. Fe_3O_4 nanoparticles were isolated and purified by centrifugation and then washed with distilled water four times to remove excess NH_4OH solution.

Cleaning of the glass slides

The glass slides were cleaned using cotton wool soaked in sodium laury sulphate. It was then sonicated in a sonicator for 1 minute to remove excess impurity there after rinsed with distilled water to remove excess fumes.

Deposition of Fe_3O_4 and Sintering of the Fe_3O_4 layer

The Fe_3O_4 liquid paste was spin-coated on the glass slide substrate with the conditions of 3000 rpm for 30 seconds. The sintering process allows the Fe_3O_4 to "melt" partially together, in order to ensure good contact and mechanical adhesion on the glass. The deposited Fe_3O_4 was dried at 250°C for 1 minute. With this one-step sintering process, it was annealed at 500°C for 30 minutes, which was beneficial to the improvement of the interfacial contact.

Preparation of Fe_3O_4/rGO

The GO was deposited on already formed Fe_3O_4 following spin coating procedure at 3000 rpm for 30 seconds.

The deposited GO on Fe_3O_4 was dried at 150°C for 5 minutes. With this one-step sintering process, it was annealed at 300°C for 30 minutes, to convert the GO to rGO.

Characterization Techniques

Optical properties of the nanocomposites were recorded using UV-Visible spectrophotometry (Axiom Medicals UV752 UV-vis-NIR). The PL curves of prepared samples' were obtained using Renishaw in PL microscope excited at a wavelength of 325 nm.

RESULTS AND DISCUSSION

Optical Absorbance Characteristics

It has been proven that UV-visible spectroscopy is an excellent informative tool to investigate the optical properties of any nanocomposite.

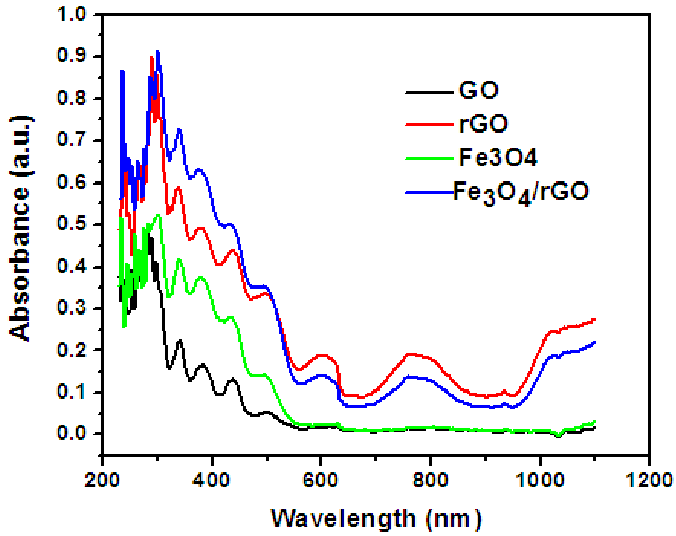

Fig. 2: Absorption spectra of GO, rGO, Fe_3O_4, Fe_3O_4/rGO

Figure 2 shows the absorption of GO, rGO, Fe_3O_4, and Fe_3O_4/rGO within the wavelength range of 200-1200 nm. From the Figure, the GO is absorbing from 240 to 630 nm with absorption peaks observed at: ~270 nm, with absorbance height of ~0.48; ~339 nm, with absorbance height of ~0.22; ~384 nm, with absorbance height of ~0.16; ~437 nm, with absorbance height of ~0.13; and ~501 nm, with absorbance height of ~0.05. We also observed rGO to have absorption peaks at 336 nm, 381 nm, 440 nm, 498 nm, 605 nm, 769 nm, and 931 nm with absorbance height around 0.58, 0.49, 0.43, 0.34, 0.19, 0.20, and 0.10 respectively. The observed absorption peak at 270 nm is expected to be attributed to the transition of aromatic C=C bonds while other peaks are expected to be related to the transition of the C=O bonds and results are in agreement with the ones obtained by Parades et al. (2008).

The Fe_3O_4 shows absorption peaks within the UV and Visible region with absorption peaks at 296, 339, 379, 434, 496, 625 nm and absorbance values at 0.51, 0.41, 0.37, 0.28, 0.14, and 0.03 respectively. The absorbance spectrum shows the absorbance is in the visible range of the wavelength. With reference to the observed peaks of Fe_3O_4 spectrum, we noticed a red shift in the spectrum of Fe_3O_4/rGO with peaks observed at 300, 339, 378, 437, 498, 605, 777, 931 nm. The shift and enhanced absorption of the Fe_3O_4/rGO nanocomposites into the longer wavelength region (visible and near infrared region) as compared to Fe_3O_4 nanoparticles and rGO, is expected to be attributed to the formation of chemical linkage between Fe_3O_4 nanoparticles and rGO after incorporation of graphene into Fe_3O_4 nanoparticles; this result is clearly in agreement with some obtained results (Phan et al., 2011, Fu et al., 2012). Hence, the presence of rGO in Fe_3O_4/rGO nanocomposite shows an excellent ability to serve as a good material for the photocatalytic performance.

.

Optical Transmission of the different as-prepared films

Figure 3 below shows the spectral transmittance curves as a function of wavelength. Transmittance is calculated from absorbance using Equation (1) (Shinen et al., 2018).

$$T(\%) = anti\log(2 - A) \quad (1)$$

Where A is absorbance and T is transmittance in %

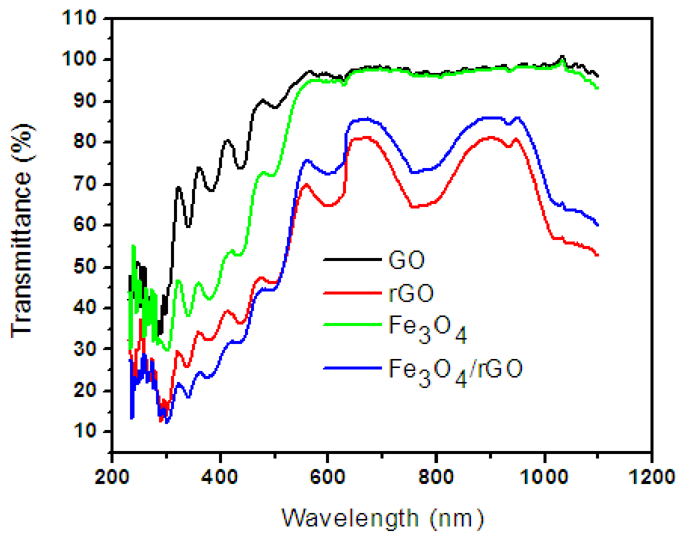

Fig. 3: Transmittance spectra of GO, rGO, Fe_3O_4, Fe_3O_4/rGO.

Figure 3 compares the optical transmission of the different as-prepared samples. The spectrum without modification as a reference is also included. It was observed that at wavelengths between 300 nm and 1000 nm, the sample with modification (Fe_3O_4/rGO) and the pure F_3O_4 have lower transmission than the sample GO. The GO and Fe_3O_4 experience a rise from 250 nm to 570 nm and maintain a constant transmission above 570 nm. At longer wavelength, for the GO and rGO films, there is a sharp rise in transmittance up to 80% within 630 to 990 nm with peaks observed at 670 nm and 970 nm, ad a valley at 780 nm. Above 990 nm and below 630 nm, we noticed a sharp fall in transmittance. The difference in observed transmittance of films may be ascribed to disparity in surface morphologies, crystallite size and existence of surface defects causing a decrease in transmittance due to incident light as described in our previous work (Bala et al., 2019).

Photoluminescence Emission Spectrum

For decade, photoluminescence (PL) emission spectrum has been considered to an extensively conducted way to study the electronic and optical properties of any photo induced semiconductor. It is based on the concepts that the faster electron transfer from the conduction band of a photo induced semiconductor to rGO sheets can prevent the recombination electron-hole rate. Figure 4 shows the obtained room temperature PL spectra of rGO, Fe_3O_4/rGO and Fe_3O_4 respectively. It was clearly observed that rGO and Fe_3O_4/rGO nanocomposites have exhibited lower PL intensity of the visible peak than that of the bare Fe_3O_4 nanoparticles (Figure 4c). Since from literature, Fe_3O_4 is found to be an indirect band-gap semiconductor with a narrow optical band gap value of 1.40 eV (Beydoun et al., 2000). This narrowed value proved to be arisen from the *d* orbitals and shows that Fe_3O_4 exhibits high electrical conductivity with almost metallic nature at room temperature. However, with the low charge carriers (electron and hole), mobility in magnetic nanoparticles may lead to an increase in electron-hole pair recombination.

Therefore, the higher PL intensity of the bare Fe_3O_4 nanoparticles is assigned to the recombination of excited electrons and holes, whereas the lower PL intensity of rGO and Fe_3O_4/rGO nanocomposites is because of the lower charge recombination rates. This shows that graphene has the tendency to greatly influence the PL intensities of Fe_3O_4/rGO nanocomposites, owing to the 2D hexagonal π-conjugation structure and excellent electronic conductivity of graphene that have the tendency to greatly influence the PL intensities of the Fe_3O_4/rGO nanocomposites.

For the rGO, it is observed to have two different carbon domains, namely sp^2 and sp^3 that has a different charge transition pathway inside each domain, respectively. Moreover, the PL emission of rGO depends on the shape, size and fractions of the sp^2 domains and sp^3 domains, thus the π-π* transition within the sp^2 carbon clusters can be attributed to the PL quenching shifting in rGO (Han et al., 2015). Amazing property such as the high charge mobility of graphene act as an electron acceptor for the photo induced electron from Fe_3O_4 nanoparticles, and eventually leads to low charge recombination rate (Liu et al., 2011).

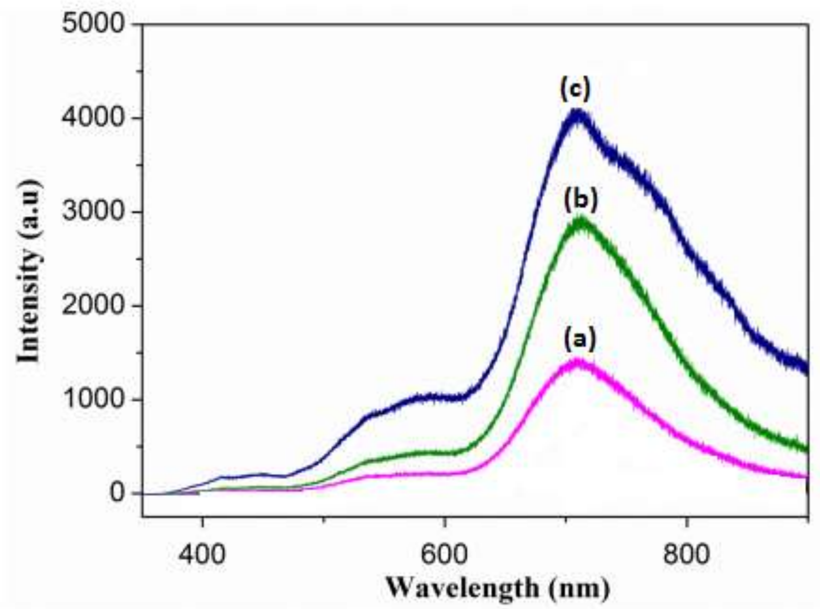

Fig. 4: Room temperature photoluminescence (PL) spectra of (a) rGO, (b)Fe_3O_4/rGO and (c) Fe_3O_4

CONCLUSION

We have successfully developed a simple, efficient, and free toxic method to synthesize Fe_3O_4/rGO nanocomposite. Our results show an enhanced response to higher wavelength, indicating an increase in visible light absorption for the UV-vis with modification of the surface. For the PL, we have found that the lower PL emission intensity of the prepared Fe_3O_4/rGO nanocomposites indicates that incorporation of electron acceptor rGO efficiently suppressed the recombination of photo induced electrons and holes pair and leading to rapid interfacial electron transfer which is more beneficial for the photocatalytic applications.

REFERENCES

Bala, D. A., Ali, H & Eli, D. (2019). Structural and morphological Properties of Reduced Graphene Oxide (rGO) on Iron Oxide Nanoparticles. Accepted for publication in *Journal of the Nigerian Society of Physical Sciences.*

Beydoun, D., Amal, R., Low, G. K.-C & McEvoy, S. (2000). Novel photocatalyst: titania-coated magnetite. Activity and photodissolution. *The Journal of Physical Chemistry B, 104*(18): 4387-4396.

Fu, Y. S., Xiong, P., Chen, H. Q., Sun, X. Q., & Wang, X. (2012). High photocatalytic activity of magnetically separable manganese ferrite-graphene heteroarchitectures. *Industrial and Engineering Chemistry Research*, 51: 725-731.

Han, F., Yang, S., Jing, W., Jiang, Z., Liu, H & Li, L. (2015). A study on NEAR-uv blue photoluminescense in graphene oxide prepared by LLangmuir-Blodgett method. *Applied Surface Science*, 345: 18-23.

Hummers Jr, W. S & Offeman, R. E. (1958). Preparation of graphitic oxide. *Journal of the American Chemical Society, 80*(6): 1339-1339.

Kemp, K. C., Seema, H., Saleh, M., Le, N. H., Mahesh, K., Chandra V & Kim. K. S. (2013). Environmental applications composites: water remediation and gas adsorption. *Nanoscale*, 5: 3149-3171.

Laurent, S., Forge, D., Port, M., Roch,A., Robic, C., Elst L.V & Muller, R. N. (2008). Magnetic iron oxide nanoparticles: synthesis, Stabilization, Vectorization, Physicochemical Characterizations, and Biological Applications. *Chemical Reviews*, 108: 2064-2110.

Li, H. B., Gui, X. C., Zhang, L. H., Wang, S. S., Ji, C. Y., Wei, J. Q., Wang, K. L., Zhu, H. W., Wu, D. H & Cao, A. Y. (2010). Carbon nanotube sponge filters for trapping nanoparticles and dye molecules from water. *Chemical Communications*, 46: 7966-7968.

Liu, X. J., Pan, L. K., Lv, T., Zhu, G., Lu, T., Sun, Z & Sun, C. Q. (2011). Microwave-assisted synthesis of TiO_2-reduced graphene oxide composites for the photocatalytic reduction of Cr(VI). *RSC Advances*, 1: 1245-1249.

Liu, Y. S; Jiang, X. Q, Li, B. J, Zhang, X. D, Liu, T. Z, Yan, X. S., Ding, J., Cai, Q and Zhang, J. M. (2014). Halloysite nanotubes@reduced graphene oxide composite for removal of dyes from water and as supercapacitors. *Journal of materials chemistry A*, 2: 4264-4269.

Maiti, U. M., Lee,W. J., Lee, J. M., Oh, Y., Kim, J. Y., Kim, J. E., Shim, J. M., Han, T. H & Kim. S. O (2014). 25th anniversary article: Chemically modified/doped carbon nanotubes & graphene for optimized nanostructures & nanodevices. *Advanced Materials*, 26(1): 40-66.

Metin, O., Aydog S & Meral, K. (2014). A new route for the synthesis of graphene oxide–Fe_3O_4 (GO-Fe_3O_4) nanocomposites and their schottky diode applications. *Journal of Alloys and Compounds*, 585: 681-688.

Novoselov, K. S., Geim, A. K., Morozov, S. V., Jiang, D., Zhang, Y., Dubonos, S. V & Firsov, A. A. (2004). Electric Field Effect in Atomically Thin Carbon Films. *Science*, 306: 666-669.

Parades, J. I., Villar-Rodil, S., Martinez-Alonso, A & Tascon J. M. D. (2008). Graphene oxide dispersions in organic solvents. *Langmuir*, 24 (19): 10560-10564.

Phan, T. D. N., Pham, V. H., Shin, E. W., Pham, H. D., Kim, S. W., Chung, J. S & Hur, S. H. (2011). The role of graphene oxide content on the adsorption-enhanced photo catalysis of titanium dioxide/graphene oxide composites. *Chemical Engineering Journal*, 170: 226- 232.

Shinen, M. H., Alsaati, S. A. A & Razooq F.Z. (2008). Preparation of high transmittance TiO_2 thin films by Sol-gel techniques as antireflection coating. *Journal of physics: conference series*, 1032,012018.

Singh, V., Joung, D., Zhai, L., Das, S., Khondaker, S.I & Seal, S. (2011). Graphene based materials: Past, present and future. *Progress in Materials Science*, 56(8): 1178-1271.

Song, X., & Gao, L. (2007). Fabrication of bifunctional titania/silicacoated magnetic spheres and their photocatalytic activities. *Journal of the American Ceramic Society*, 90(12): 4015–4019.

Wang, Y. Bai, Y. J., Li, X., Feng Y.Y & Zhang, H. J. (2013). A general strategy towards encapsulation of nanoparticles in Sandwiched graphene sheets and the synergic effect on energy story. *Chemistry–A European journal*, 19: 3340-3347.

Wu, Q. H., Feng, C., Wang, C., & Wang, Z. (2013). A facile one-pot solvothermal method to produce superparamagnetic graphene-Fe_3O_4 nanocomposite and its application in the removal of dye from aqueous solution. *Colloids and Surfaces B: Biointerfaces*, 101: 210-214.